Virologica Sinica 39 (2024) 31–43

Contents lists available at ScienceDirect

Virologica Sinica

journal homepage: www.keaipublishing.com/en/journals/virologica-sinica
www.virosin.org

Research Article

Ancient dormant virus remnant ERVW-1 drives ferroptosis via degradation of GPX4 and SLC3A2 in schizophrenia

Dongyan Zhang [a], Xiulin Wu [a], Xing Xue [a], Wenshi Li [a], Ping Zhou [a], Zhao Lv [a], Kexin Zhao [a], Fan Zhu [a,b,*]

[a] State Key Laboratory of Virology and Department of Medical Microbiology, School of Basic Medical Sciences, Wuhan University, Wuhan, 430071, China
[b] Hubei Province Key Laboratory of Allergy & Immunology, Wuhan University, Wuhan, 430071, China

ARTICLE INFO

Keywords:
ERVW-1
Glutathione peroxidase 4 (GPX4)
Solute carrier family 3 member 2 (SLC3A2)
Ferroptosis
Schizophrenia

ABSTRACT

Human endogenous retroviruses (HERVs) are remnants of retroviral infections in human germline cells from millions of years ago. Among these, ERVW-1 (also known as HERV-W-ENV, ERVWE1, or ENVW) encodes the envelope protein of the HERV-W family, which contributes to the pathophysiology of schizophrenia. Additionally, neuropathological studies have revealed cell death and disruption of iron homeostasis in the brains of individuals with schizophrenia. Here, our bioinformatics analysis showed that differentially expressed genes in the human prefrontal cortex RNA microarray dataset (GSE53987) were mainly related to ferroptosis and its associated pathways. Clinical data demonstrated significantly lower expression levels of ferroptosis-related genes, particularly Glutathione peroxidase 4 (GPX4) and solute carrier family 3 member 2 (SLC3A2), in schizophrenia patients compared to normal controls. Further in-depth analyses revealed a significant negative correlation between ERVW-1 expression and the levels of GPX4/SLC3A2 in schizophrenia. Studies indicated that ERVW-1 increased iron levels, malondialdehyde (MDA), and transferrin receptor protein 1 (TFR1) expression while decreasing glutathione (GSH) levels and triggering the loss of mitochondrial membrane potential, suggesting that ERVW-1 can induce ferroptosis. Ongoing research has shown that ERVW-1 reduced the expression of GPX4 and SLC3A2 by inhibiting their promoter activities. Moreover, Ferrostatin-1 (Fer-1), the ferroptosis inhibitor, reversed the iron accumulation and mitochondrial membrane potential loss, as well as restored the expressions of ferroptosis markers GSH, MDA, and TFR1 induced by ERVW-1. In conclusion, ERVW-1 could promote ferroptosis by downregulating the expression of GPX4 and SLC3A2, revealing a novel mechanism by which ERVW-1 contributes to neuronal cell death in schizophrenia.

1. Introduction

Human endogenous retroviruses (HERVs) are remnants of ancient exogenous retroviruses that integrated into the human genome millions of years ago by infecting germline cells (Li et al., 2022; Yu et al., 2013). HERVs are polynucleotide sequences with a complete retrovirus structure, accounting for approximately 8% of the human genome and replicating along with the human genome through Mendel's law (Kury et al., 2018). Most HERVs are defective, contain major deletions or nonsense mutations, and have become part of the host genome (Markovitz, 2014). Only a few HERVs have complete open reading frames (ORFs) that encode functional proteins (Grandi et al., 2018a). These full-length HERVs possess general components of retroviruses, including two long terminal repeats (LTRs), GAG, POL (retroviral polymerase gene), and ENV (envelope) (Yu et al., 2013). HERVs are divided into three classes based on the sequence similarity of their pol regions, namely, class I (Gammaretrovirus), II (Betaretrovirus), and III (Spumaretrovirus) (Vargiu et al., 2016).

HERVs play crucial roles in processes such as placental syncytiotrophoblast formation, antiviral immune defense, and gene transcription (Grandi et al., 2018b; Mao et al., 2021; Song et al., 2021). Typically, HERVs are not expressed or have low transcriptional activity due to epigenetic regulation. However, many factors can reactivate the expression of HERVs, including environmental stimuli such as drugs (e.g., caffeine and aspirin) (Liu et al., 2013) and exogenous radiation (Lee et al., 2012), infectious factors like viral infections (e.g. human cytomegalovirus (Illescas-Montes et al., 2019) and hepatitis B virus (Liu et al., 2017)), and internal factors such as aging-associated processes

* Corresponding author.
E-mail addresses: fanzhu@whu.edu.cn, zhufan@hotmail.com (F. Zhu).

https://doi.org/10.1016/j.virs.2023.09.001
Received 4 May 2023; Accepted 6 September 2023
Available online 9 September 2023

(Nevalainen et al., 2018) and epigenetics changes (Garcia-Montojo et al., 2018). Activated HERVs may be involved in certain diseases, such as certain cancers (Jansz et al., 2021; Yu et al., 2013), autoimmune diseases (Posso-Osorio et al., 2021), and neuropsychiatric disorders (Li et al., 2023; Yao et al., 2023).

The HERV-W family, which accounts for nearly 1% of the human genome, is the oldest HERV family and belongs to Class I transposons (Gifford et al., 2018). The envelope protein gene (ERVW-1, also known as HERV-W-ENV, ERVWE1, or ENVW), located on chromosome 7, encodes a protein called Syncytin-1. This protein, mainly expressed in the human placenta, is involved in syncytium formation and trophoblast cell fusion (Garcia-Montojo et al., 2020). Emerging evidence indicates that ERVW-1 is associated with a variety of diseases, including autoimmune diseases (Mameli et al., 2007), cancers (Yu et al., 2014; Zhou et al., 2021), and neuropsychiatric disorders (Kury et al., 2018; Wang et al., 2018). Notably, previous research has shown that ERVW-1 is abnormally elevated in patients with schizophrenia (Huang et al., 2011; Li et al., 2023; Wu et al., 2023; Xia et al., 2021; Yan et al., 2022; Yao et al., 2023).

Schizophrenia is a chronic brain disease that affects approximately 1% of the world's population, posing a significant health and economic burden on society (Marder et al., 2019). Biochemical theories indicate that schizophrenia is primarily caused by an imbalance of neurotransmitters in the brain, including dopamine, glutamate, serotonin, and acetylcholine, with the hypothesis of abnormal glutamate metabolism playing a key role in the neuropsychology of schizophrenia (Stepnicki et al., 2018). Glutamate, a major excitatory neurotransmitter, weakens the ability of cysteine/glutamate antiporter system Xc-to transport cysteine into cells, leading to reduced intracellular levels of antioxidant glutathione and neurotoxicity (Bridges et al., 2012). The cystine/glutamate transporter system Xc-is critical in glutamate metabolism and consists of a light-chain subunit (xCT, SLC7A11) and a heavy-chain subunit (CD98hc, SLC3A2) (Koppula et al., 2021). The SLC3A2 gene, encoding the transmembrane glycoprotein CD98 (Vection et al., 2022), is downregulated in schizophrenia (Lin et al., 2016). Moreover, studies have shown that patients with schizophrenia may exhibit abnormal antioxidant protection mechanisms in cerebrospinal fluid (CSF) and postmortem brain tissue (Lin et al., 2016). The downregulation of SLC3A2 and the imbalance of antioxidants are key features of ferroptosis.

Ferroptosis is a form of cell death driven by iron-dependent lipid peroxidation, representing a new type of programmed cell death distinct from apoptosis, cell necrosis, and autophagy (Dixon et al., 2012). It involves the consumption of unsaturated fatty acids within the plasma membrane and the accumulation of iron-induced lipid reactive oxygen species, leading to oxidative stress response in cells and causing fatal damage to proteins, nucleic acids, and lipids, ultimately resulting in cell death (Zhang et al., 2022). Three main factors are involved in cell death through ferroptosis: the increase of intracellular free iron, the depletion of redox glutathione/GPX4/system Xc-axis, and the oxidation of membrane polyunsaturated fatty acids (PUFAs) (Jiang et al., 2021). Ferroptosis influences diverse diseases, such as degenerative diseases, cancers, cardiovascular and cerebrovascular diseases, ischemia-reperfusion injury, and renal degeneration (Yan et al., 2021). Ferroptosis is particularly crucial in several neurological diseases, including Parkinson's disease (Zhang et al., 2022) and Alzheimer's disease (Wang et al., 2022). However, the relationship between ferroptosis and schizophrenia remains unclear.

In this study, our bioinformatics analysis of the RNA microarray dataset GSE53987 from the human prefrontal cortex showed that differentially expressed genes were predominantly involved in ferroptosis and its related pathways. Our clinical data suggested significantly reduced expression levels of ferroptosis-related genes GPX4 and SLC3A2, which were significantly negatively correlated with ERVW-1 in schizophrenia patients. *In vitro* studies suggested that ERVW-1 induced ferroptosis and the ferroptosis inhibitor Ferrostatin-1 (Fer-1) could counteract the effect induced by ERVW-1. Further studies showed that ERVW-1 decreased the transcription and protein levels of GPX4 and SLC3A2. Luciferase assay showed that ERVW-1 inhibited the activity of the GPX4 and SLC3A2 promoters. In summary, our findings suggest that ERVW-1 could promote ferroptosis by downregulating the expression of GPX4 and SLC3A2, implicating ferroptosis as a potential novel risk factor for schizophrenia.

2. Materials and methods

2.1. Clinical samples and ethical considerations

The blood samples from patients with schizophrenia and healthy controls were obtained from the Renmin Hospital, Wuhan University. All patients met the symptoms of schizophrenia-related psychosis of recent onset, as defined in the fifth edition of the Diagnostic and Statistical Manual of Mental Disorders (American Psychiatric Association, 2013). None of the 47 patients had any history of antipsychotic drug treatment or exhibited acute infectious, inflammatory, or nervous system disease symptoms. Thirty-six healthy controls were healthy donors. All plasma samples were mixed with ethylenediamine tetraacetic acid and immediately stored at −80 °C until the end of the experiment. There were no significant differences in median age, education level, body mass index, smoking status, and gender distribution between controls and patients with schizophrenia.

2.2. Bioinformatics

We obtained the human prefrontal cortex gene expression profile of GSE53987 in the GPL570 platform (Affymetrix Human Genome U133 Plus 2.0 Array) with schizophrenic and normal individuals (Lanz et al., 2019). Microarray data were downloaded from the GEO query. We utilized Sanger box online tools (Shen et al., 2022) to present differentially expressed genes (DEGs) by Volcano plots and heat maps. In addition, we used the Sanger box to visualize the DEGs' enrichment of KEGG and gene ontology (GO) biology biological processes ($P < 0.05$). We showed the expression of three genes (ERVW-1, GPX4, and TFRC) between patients and normal controls by using the Wilcoxon test with ggplot2 (R package).

2.3. ELISA assay

As recommended by the manufacturer's recommendation, the expression level of human ERVW-1 (Liberi Bio, LB111222B, Wuhan, China), SLC3A2 (Liberi Bio, LB11168B; Wuhan China), and GPX4 (Liberi Bio, LB9483B; Wuhan, China) in serum was determined with ELISA kit. Use a Multiskan FC plate reader to measure the absorbance at 450 nm.

2.4. Plasmid construction

The previously obtained ERVW-1 sequence (Huang et al., 2011) was cloned into the mammalian expression vector pcDNA 3.1 vector. The human GPX4 (NM_002085.5) and SLC3A2 (NM_001012662.3) genes were amplified according to the sequence of the genes in the National Center for Biotechnology Information (Bethesda, MD, United States). The genes were then cloned into the pCMV-T7-MCS-3 × FLAG-WPRE-Neo vector (miaolingbio, P39495, China). For luciferase assay, human SLC3A2 promoters (−588 to +212, −388 to +212, −188 to +212, and +12 to +212) and GPX4 promoters (−700 to +100, −500 to +100, −300 to +100, and −100 to +100) were cloned into the luciferase reporter vector pGL3-basic vector, which contains a firefly luciferase gene. All primers were designed using Premier 5.0 and described in Supplementary Table S1. All constructs were confirmed by sequencing (Sangon Biotech, Shanghai, China).

2.5. Cell culture and transfection

The human neuroblastoma cell line SH-SY5Y (CRL-2266) was purchased from the American Type Culture Collection (ATCC, Manassas, VA,

USA). Cell lines were cultured in a 1:1 mixture of Minimal Essential Medium (MEM) (Gibco, 2225320, Newyork, CA, USA) and F12 Media (Gibco, 2209586, Newyork, CA, USA) supplemented with 10% heat-inactivated fetal bovine serum (Biological Industries, 2001003, Beit HaEmek, Israel). All cell cultures were supplemented with 1% penicillin/streptomycin (Gibco, 15140148, Newyork, CA, USA) and 100 mmol/L sodium pyruvate (Gibco, 2185865, Newyork, CA, USA) mixed with 5% CO_2 at 37 °C. According to the manufacturer's instructions, the LipofectamineTM2000 transfection reagent (Invitrogen, 11668030, Carlsbad, CA, USA) was used for transfection. Cells were harvested 24, 36, and 48 h after transfection for further studies.

2.6. Analysis of mRNA expression

Total RNA was isolated from cultured cells using TRIzol reagent (Invitrogen, Carlsbad, CA, USA). Genomic DNA contamination from total RNA was removed using DNase I (Thermo, EN0521, Waltham, MA, USA) according to the manufacturer's recommendation, followed by the MMLV Reverse Transcriptase cDNA Synthesis Kit (Invitrogen, 18091200, Carlsbad, CA, USA) for reverse transcription. Real-time Quantitative Polymerase Chain Reaction (q-PCR) was performed on an iCycler system (Bio-Rad, Hercules, CA, USA)® using SYBR Select Master Mix (Invitrogen, Carlsbad, CA, US). Actin was used as a housekeeping gene to normalize gene expression. Primer designs were based on sequences obtained from the NCBI database using Primer 5.0 software and are listed in Supplementary Table S1.

2.7. Western blot analysis

Proteins were extracted from cultured cells lysed with mammalian protein extraction reagent (Thermo, 78505, Waltham, MA, USA) and protease inhibitor mixture (Sigma, P8340, Steinheim, Germany), and the protein concentrations were measured with a BCA protein detection kit (Thermo, 23250, Waltham, MA, USA). Proteins were separated by 12% SDS-PAGE and then imprinted onto PVDF membranes (Millipore, USA). Then, the primary antibody: anti-SLC3A2 antibody (Zenbio, 383101, China), anti-GPX4 antibody (ABclonal, A11243, USA), anti-ERVW-1 antibody (ABclonal, A16522, USA), and anti-actin antibody (Abcam, ab8226, USA) were incubated with 5% skim milk in TBST. After overnight incubation, the secondary antibody (HRP-conjugated anti-rabbit) was added to the membrane, followed by color observation with the ECL kit (Millipore, USA) and images captured with the Tanon 5200 chemiluminescence imaging system (Tanon, Shanghai, China) for analysis. Expression levels of target proteins were normalized to actin.

2.8. Iron assay

Intracellular ferrous content was determined using iron content determination (Abcam, ab83366, USA) according to the manufacturer's instructions. First, samples were collected, washed with cold PBS, homogenized, mixed, and incubated in the assay buffer. Iron probe was added to the iron standard and test sample Wells, mixed, and incubated at 37 °C in the dark for 60 min. The content was immediately measured on a Multiscan FC plate reader (absorbance OD 593 nm).

2.9. Glutathione assay

According to the manufacturer's instructions, the glutathione concentration was measured using the GSH and GSSG assay kit (Beyotime, S0053, China). GSSG is reduced to GSH by glutathione reductase, which can react with the chromogenic substrate DTNB to form yellow TNB and GSSG. The amount of total glutathione could be calculated by measuring the content of 412 nm on the Multiskan FC plate reader (Thermo Scientific, Waltham, MA, USA).

2.10. MDA assay

Cell samples were prepared as described in the lipid peroxide MDA Assay kit (Beyotime, S0131, China). The MDA level was detected at 532 nm by Multiskan FC plate reader.

2.11. Flow cytometry

Flow cytometry was used to detect mitochondrial membrane potential and identify TFR1-positive cells. Cell suspensions were prepared as described in the mitochondrial membrane Potential Assay kit (Beyotime, S2001, China). After staining with TMRE staining working solution, cells were incubated at 37 °C for 30 min, and detected with an Epics Altra II cell analyzer (Beckman Coulter, Miami, FL, USA). FlowJo software (Tree star, Ashland Inc, USA) was used for analysis.

Collection 1×10^6 cells were suspended in 5% BSA, and treated with ABfloTM 488 rabbit anti-human CD71 monoclonal antibody (A22301, ABclone) for 30 min to detect TFR1-positive cells.

2.12. Luciferase activity assay

According to the Dual-Luciferase Reporter Assay Kit (Vazyme, DL101, China), a dual luciferase assay system with Renilla luciferase as an internal parameter was used to correct the transfection efficiency, and the luciferase activity of the reporter gene firefly was detected. The plasmids and target genes were co-transfected into SH-SY5Y cells for 24 h at 37 °C and 5% CO_2, and luciferase activity was measured. Promoter activity was expressed as the mean ± standard deviation (SD) of at least three replicates.

2.13. Drug treatment

Ferrostatin-1 (#HY-100579, MCE, NJ, USA) was diluted in dimethyl sulfoxide (DMSO) to a 20 mmol/L concentration. Ferrostatin-1 was added to the medium at serial dilutions or a given concentration after plasmid transfection. Cells were grown for 24–48 h before assessing other markers.

2.14. Statistical analysis

SPSS13.0 and GraphPad Prism were used for statistical analysis. Median analysis and Mann-Whitney U analysis were performed on clinical samples to compare the differential expression of ERVW-1, SLC3A2, and GPX4 between schizophrenia and control groups. Spearman rank correlation was used for correlation analysis. All data were obtained from at least three independent experiments. One-way ANOVA and Student's *t*-test were used for statistics and data analysis. The minimum level of statistical significance was set at $P < 0.05$.

3. Results

3.1. Low levels of GPX4 and SLC3A2 in schizophrenia and their correlation with ERVW-1

GEO databases are commonly used to explore new avenues in disease diagnosis and treatment (Kourou et al., 2015). We analyzed a schizophrenia RNA microarray dataset, GSE53987, from the human prefrontal cortex in the GEO database. The microarray results revealed 2237 upregulated genes and 4963 downregulated genes (Fig. 1A). The expression values of the top 200 genes with the most significant differences are shown in the heat map (Fig. 1B). The differentially expressed genes (DEGs) analyzed by KEGG focused on the ferroptosis pathway and its related pathways such as glutamatergic synapse, p53 signaling pathway, and fatty acid metabolism (Fig. 1C). Additionally, GO biological processes enrichment analysis showed that DEGs were predominantly enriched in several biological pathways, including lipid metabolic

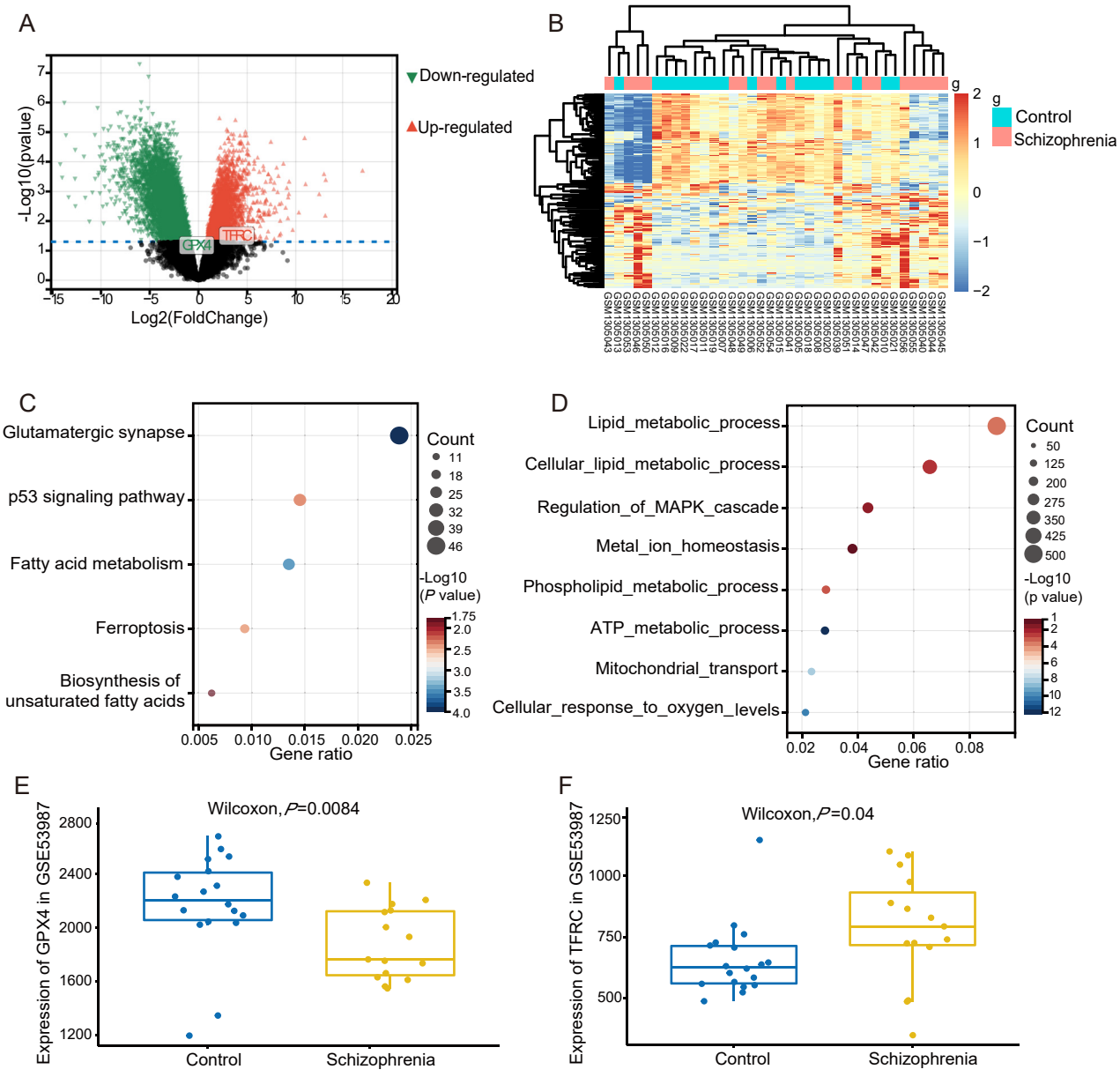

Fig. 1. Schizophrenia is associated with ferroptosis according to bioinformatics. **A** The volcano plot of each gene expression profile data and differentially expressed genes identified using R software. **B** The heat map of 200 DEGs with the most significant differences. **C** KEGG analyses of the DEGs. **D** GO analysis of DEGs. The level of GPX4 (**E**) and TFRC (**F**) in GSE53987.

process, regulation of MAPK cascade, metal ion homeostasis, ATP metabolic process, mitochondrial transport, and cellular response to oxygen levels (Fig. 1D). Further analysis of GSE53987 indicated that GPX4 levels were lower in people with schizophrenia than in the control group (Fig. 1E). In contrast, transferrin receptor (TFRC, also known as transferrin receptor protein 1, TFR1) levels were higher than in the control group (Fig. 1F). Besides, there was an elevated expression of ERVW-1 in GSE53987 data set (Supplementary Fig. S1).

Schizophrenia is a heterogeneous disorder with complex clinical manifestations, which limits its diagnosis (Tandon et al., 2013). The study of serum biomarkers is helpful for the diagnosis of schizophrenia (Mohammadi et al., 2018). Our bioinformatics results suggested GPX4 as a potential biomarker for schizophrenia. Moreover, we found that the serum GPX4 level in patients was about 40% lower than in normal controls (Fig. 2A), aligning with the prediction of bioinformatics in GSE53987. The inhibition of system Xc-leads to GSH downregulation and GPX4 inhibition (Stockwell, 2022). Therefore, we measured SLC3A2 levels in blood samples from both schizophrenia patients and healthy individuals. The results showed that the serum SLC3A2 level was about 25% lower in patients than in healthy people (Fig. 2B). Using the Spearman rank correlation method for correlation analysis, we found a positive correlation between SLC3A2 and GPX4 (Fig. 2C; $r = 0.57$). ELISA of blood samples revealed higher ERVW-1 levels in schizophrenia patients (Fig. 2D), consistent with our previous study (Huang et al., 2011; Li et al., 2023; Wang et al., 2018; Wu et al., 2023; Xia et al., 2021; Yan et al., 2022; Yao et al., 2023). Furthermore, Spearman's analysis showed that ERVW-1 negatively correlated with GPX4 (Fig. 2E; $r = -0.64$) in the serum of patients with schizophrenia. Meanwhile, Spearman analysis showed a negative correlation between ERVW-1 and SLC3A2 in the serum of schizophrenia patients (Fig. 2F; $r = -0.56$).

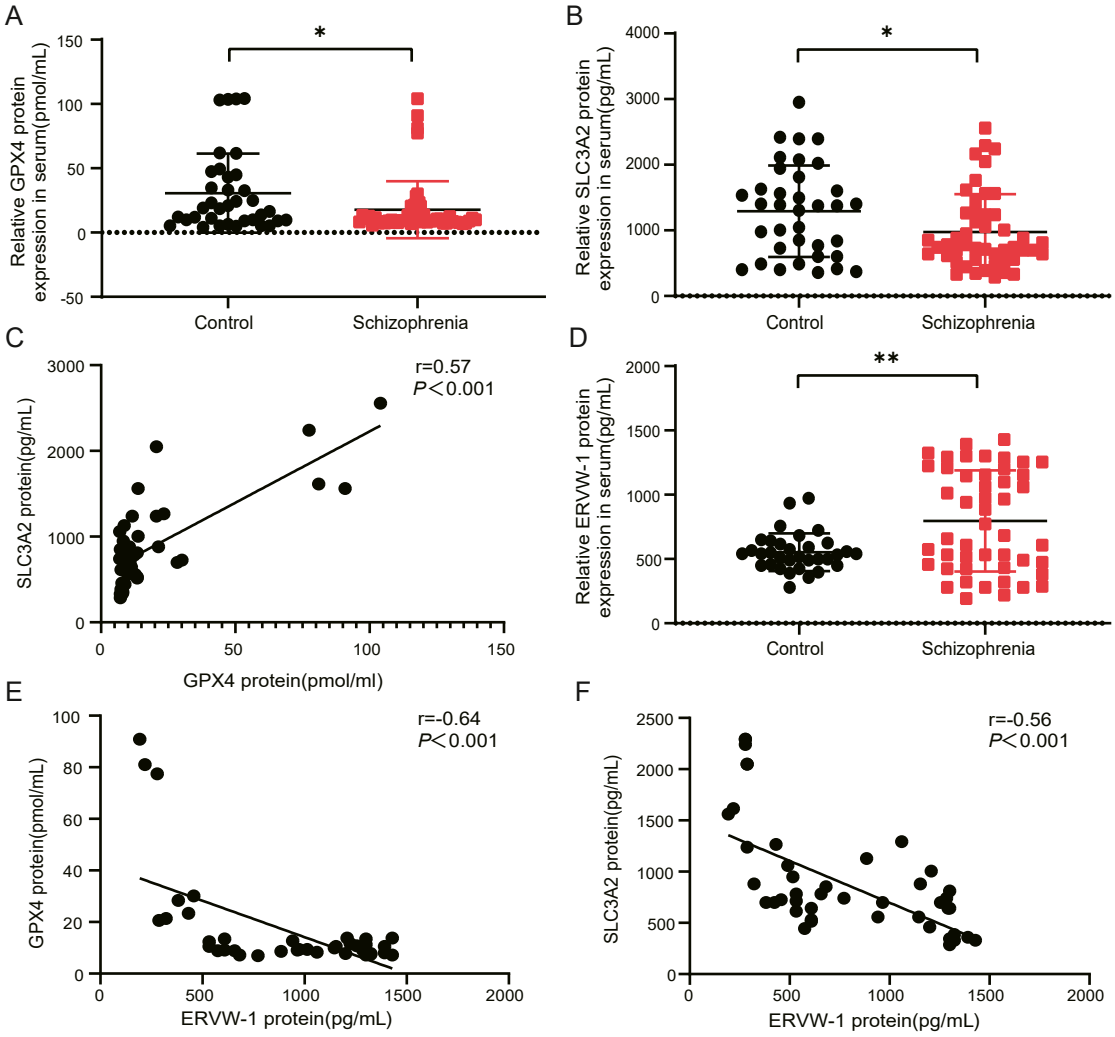

Fig. 2. GPX4 and SLC3A2 dynamics in schizophrenia patients and their correlation with ERVW-1. The concentration of GPX4 (**A**), SLC3A2 (**B**), and ERVW-1 (**D**) in healthy controls (N = 36) and schizophrenia (N = 47) by ELISA. $^{*}P < 0.05$, $^{**}P < 0.01$. **C, E, F** Correlation between SLC3A2, GPX4, and ERVW-1 expression levels in schizophrenia by Spearman's analysis. X-axis: the concentration of GPX4 or ERVW-1; Y-axis: the concentration of SLC3A2 or GPX4.

In conclusion, both GPX4 and SLC3A2, which negatively correlated with ERVW-1 in patients with schizophrenia, might serve as potential blood biomarkers and possible pathogenic factors for schizophrenia.

3.2. *ERVW-1 induces ferroptosis*

Fe^{2+} can directly produce excessive reactive oxygen species (ROS) through the Fenton reaction, thereby promoting ferroptosis (Zhang et al., 2022). Our results manifested that ERVW-1 significantly increased intracellular free Fe^{2+} by about 26% in SH-SY5Y cells (Fig. 3A and B). Fer-1 is a synthetic antioxidant that inhibits ferroptosis by preventing damage to membrane lipids through a reductive mechanism (Miotto et al., 2020; Tang et al., 2021). Interestingly, the increase in free Fe^{2+} levels caused by ERVW-1 was significantly attenuated following Fer-1 treatment (Fig. 3C). Besides, GSH, a scavenger of free radical reactive oxygen species (ROS), regulates cell metabolism and suppresses ferroptosis (Ursini et al., 2020). ERVW-1 significantly downregulated intracellular GSH by about 26% in SH-SY5Y cells (Fig. 3D). Fer-1 treatment significantly counteracted the GSH depletion induced by ERVW-1 (Fig. 3E). Malondialdehyde (MDA) is a reactive aldehyde after lipid peroxidation, one of the critical indexes of ferroptosis (Stockwell, 2022). We found that ERVW-1 significantly increased the cellular MDA by about 25% in SH-SY5Y cells (Fig. 3F). While MDA was significantly downregulated under Fer-1 treatment (Fig. 3G).

Furthermore, changes in mitochondrial morphology occur during ferroptosis, including mitochondrial shrinkage, cristae enlargement, and outer membrane rupture (Stockwell, 2022). We found that mitochondrial membrane potential (MMP) decreased by 44% in SH-SY5Y cells after ERVW-1 overexpression (Fig. 3H), representing the loss of cell membrane potential. We also found that Fer-1 restrained the ERVW-1-induced downregulation of mitochondrial membrane potential (Fig. 3I). Finally, TFR1 is another crucial indicator of ferroptosis, which enhances the ferroptosis by additional uptake of iron-carrying transferrin (Stockwell, 2022). ERVW-1 significantly upregulated TFR1 by about 53% in SH-SY5Y cells (Fig. 3J). Notably, Fer-1 significantly downregulated TFR1 expression triggered by ERVW-1 (Fig. 3K).

These results indicated that the ferroptosis inhibitor Fer-1 reversed the effect of ERVW-1 on ferroptosis-related indexes, confirming the ability of ERVW-1 to instigate ferroptosis.

3.3. *ERVW-1 reduces the expression of GPX4 and SLC3A2*

Clinical data suggested interrelationships among the expression levels of ERVW-1, SLC3A2, and GPX4 genes in schizophrenia. Successful

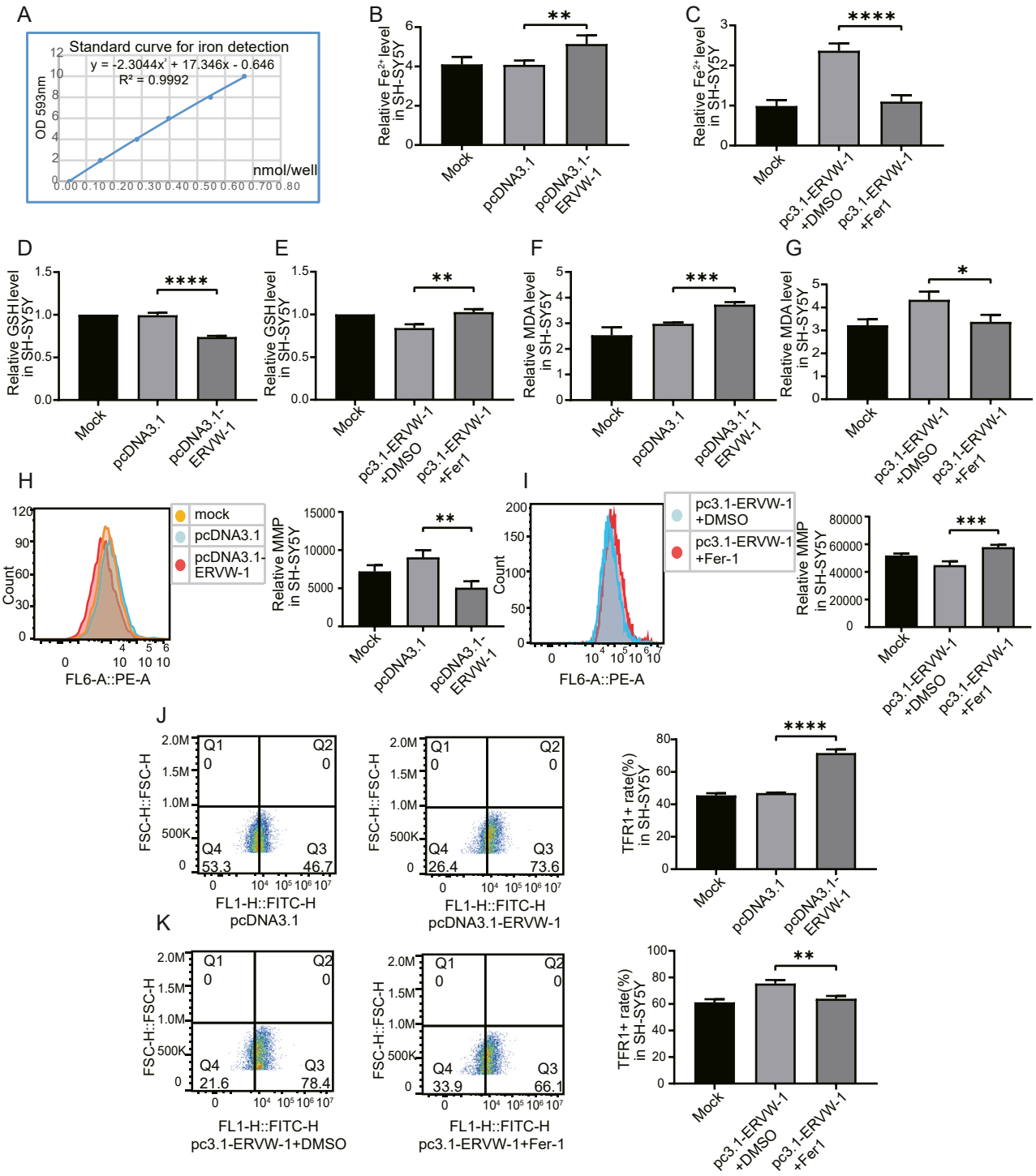

Fig. 3. ERVW-1 induced ferroptosis. **A** Standard curve of Fe^{2+} detection. **B** ERVW-1 upregulated Fe^{2+} levels in SH-SY5Y cells. **C** Fer-1 reversed the effect of ERVW-1 on Fe^{2+}. **D** ERVW-1 downregulated GSH levels in SH-SY5Y cells. **E** Fer-1 reversed the downregulation of GSH induced by ERVW-1. **F** ERVW-1 upregulated MDA levels in SH-SY5Y cells. **G** MDA was significantly downregulated under Fer-1 treatment. **H** ERVW-1 reduced mitochondrial membrane potential in SH-SY5Y cells. **I** Fer-1 restrained the ERVW-1-induced downregulation of mitochondrial membrane potential. **J** ERVW-1 increased TFR1 expression in SH-SY5Y cells. **K** Fer-1 downregulated TFR1 expression that induced by ERVW-1. Each experiment was repeated three times. Data shown are mean ± SD. Statistical analysis was performed by one-way analysis of variance (ANOVA). $^{*}P < 0.05$, $^{**}P < 0.01$, $^{***}P < 0.001$.

ERVW-1 transfection was confirmed by validation using qPCR and Western blot analysis (Supplementary Fig. S2). We found that ERVW-1 decreased mRNA levels of GPX4 (Fig. 4A) and SLC3A2 (Fig. 4B). ERVW-1 also reduced the protein levels of GPX4 (Fig. 4C) and SLC3A2 (Fig. 4D), but exerted no influence on SLC7A11 expression (Supplementary Fig. S3). Moreover, our results showed that Fer-1 did not notably alter the expression of GPX4 and SLC3A2 proteins (Supplementary Fig. S4).

Typically, promoters are crucial in regulating gene expression (Danino et al., 2015). We isolated the genomic DNA segments (ranging from −700 to +100) of the promoter region of the GPX4 gene with the transcription start site (TSS) as 0 and ligated it to the Luciferase reporting

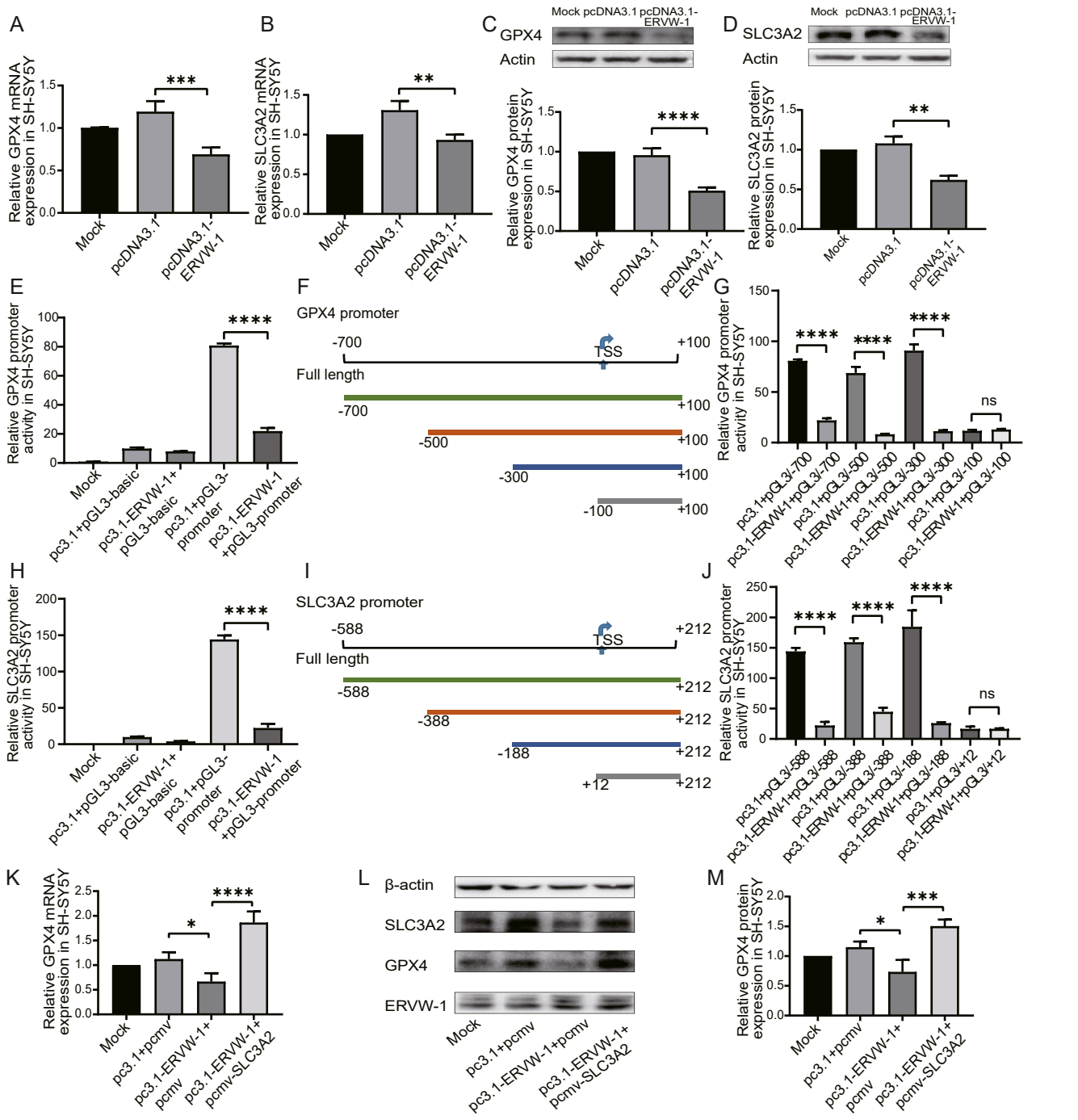

Fig. 4. ERVW-1 downregulated the expression of GPX4 and SLC3A2 by inhibiting their promoter activity. **A, B** The downregulation of GPX4 and SLC3A2 in ERVW-1-transfected SH-SY5Y cells was validated by RT-qPCR. **C, D** The downregulation of GPX4 and SLC3A2 in ERVW-1-transfected SH-SY5Y cells was validated by Western blot. **E** Luciferase assays of pGL3-GPX4 promoter co-transfected with pcDNA3.1-ERVW-1 or control vector in SH-SY5Y cells. **F** Construction of different lengths of pGL3-GPX4 promoter plasmid. **G** Luciferase assays of different lengths of pGL3-GPX4 promoter co-transfected with pcDNA3.1-ERVW-1 or control vector in SH-SY5Y cells. **H** Luciferase assays of pGL3-SLC3A2 promoter co-transfected with pcDNA3.1-ERVW-1 or control vector in SH-SY5Y cells. **I** Construction of different lengths of pGL3-SLC3A2 promoter plasmid. **J** Luciferase assays of different lengths of pGL3-SLC3A2 promoter co-transfected with pcDNA3.1-ERVW-1 or control vector in SH-SY5Y cells. **K, L, M** SLC3A2 significantly increased the ERVW-1-induced downregulation of GPX4 mRNA and protein. Data shown are mean ± SD. $^{*}P < 0.05$, $^{**}P < 0.01$, $^{***}P < 0.001$; one-way ANOVA.

vector. Luciferase experiments presented that ERVW-1 mediated suppression of GPX4 promoter activity (Fig. 4E). Subsequent experiments with four truncated promoter constructs (Fig. 4F) revealed that the sequence between −300 and + 100 was requisite for maintaining GPX4 transcriptional regulation (Fig. 4G). Similarly, we also isolated the genomic DNA fragments (ranging from −588 to +212) of the promoter region of the SLC3A2 gene. Luciferase experiments demonstrated the inhibitory effect of ERVW-1 on SLC3A2 promoter activity (Fig. 4H). We

constructed four sequence-truncated promoter plasmids of SLC3A2 (Fig. 4I), and luciferase reporter analysis revealed promoter sequences ranging from −188 to +212, the minimal sequence required for biological activity (Fig. 4J). In addition, Successful SLC3A2 transfection was confirmed by qPCR and Western blot analysis (Supplementary Fig. S5). SLC3A2 overexpression reversed the ERVW-1-induced downregulation of GPX4 mRNA and protein in SH-SY5Y cells (Fig. 4K, L and M). These results suggested that ERVW-1 could downregulate the expression of GPX4 and SLC3A2 by impeding their promoter activity.

3.4. ERVW-1 induces ferroptosis by downregulating the expression of GPX4 and SLC3A2

GPX4 is crucial in ferroptosis (Ursini et al., 2020). Given the strong correlation between ERVW-1 and GPX4 from clinical data, we constructed a GPX4 overexpression vector to investigate the role of GPX4 in ERVW-1-induced ferroptosis. The subsequent assessment revealed that overexpression of GPX4 in SH-SY5Y cells could reverse the ERVW-1-induced elevation in free Fe^{2+} levels (Fig. 5A). Besides, GPX4 resulted in a rebound in GSH downregulation prompted by ERVW-1 (Fig. 5B). In addition, GPX4 significantly neutralized the ERVW-1-induced surge in MDA levels (Fig. 5C). Furthermore, GPX4 led to a notable augmentation of mitochondrial membrane potential (Fig. 5D). Finally, GPX4 effectively reversed the upregulation of TFR1 triggered by ERVW-1 (Fig. 5E).

System Xc-/GSH/GPX4 is a central regulatory pathway for ferroptosis (Liu et al., 2022). Intriguingly, we found that SLC3A2 reversed the ERVW-1-induced suppression of GPX4 expression (Fig. 4K-M). This insight drove us to construct a SLC3A2 overexpression plasmid to explore the role of SLC3A2 in ERVW-1-induced ferroptosis. We found that SLC3A2 negated the ERVW-1-driven rise in free Fe^{2+} levels (Fig. 6A) and thwarted the GSH depletion caused by ERVW-1 (Fig. 6B). In addition, SLC3A2 significantly inhibited the trend of ERVW-1-induced MDA upregulation (Fig. 6C). Furthermore, SLC3A2 impeded the mitochondrial membrane potential decrement induced by ERVW-1 (Fig. 6D). Finally, SLC3A2 could significantly restrain the upregulation of TFR1 caused by ERVW-1 (Fig. 6E). In conclusion, ERVW-1 appeared to instigate ferroptosis by inhibiting the expression of GPX4 and SLC3A2.

4. Discussion

HERVs contribute to development of various disorders through multiple mechanisms (Geis et al., 2020; Zhang et al., 2022), such as assembling viral particles (Wang et al., 2018), generating HERV-derived lncRNAs (Zhou et al., 2019) and dsRNAs (Canadas et al., 2018), acting as promoters or enhancers to regulate cellular gene expression through LTR *cis*-regulatory element (Yu et al., 2013), or encoding viral proteins to regulate host cell signaling networks (Li et al., 2023; Wang et al., 2018; Wu et al., 2023; Xia et al., 2021; Yan et al., 2022; Yao et al., 2023). Abnormal expression of ERVW-1 has been linked to schizophrenia (Huang et al., 2011; Xia et al., 2021; Yan et al., 2022), and further studies have shown that ERVW-1 induces inflammatory abnormalities, including promoting NO release (Xiao et al., 2017), activating TLR3 signaling pathway (Wang et al., 2018, 2021), promoting cytotoxic T lymphocyte (CTL) responses of glial cells (Tu et al., 2017), and inducing innate immune activation by upregulating IFN-β, thereby mediating neuronal apoptosis (Li et al., 2023). In addition, ERVW-1 can directly activate Na^{+} (Wu et al., 2023), Ca^{2+} (Chen et al., 2019), or K^{+} (Li et al., 2013; Wu et al., 2023) ion channels, contributing to the pathophysiology of schizophrenia. In addition, our study reveals that ERVW-1 leads to neuronal dysfunction and abnormal morphology, including causing mitochondrial complex I defect in neurons to impair neuronal energy metabolism (Xia et al., 2021), triggering dopaminergic neuronal abnormalities through dopamine receptor D2 (DRD2) risk for schizophrenia (Yan et al., 2022), inhibiting hippocampal neuronal morphology and dendritic spine density by restraining the Wnt/JNK noncanonical pathway (Yao et al., 2023), and inducing the dysregulation of homeostasis in the endoplasmic reticulum (ER) (Xue et al., 2023). Continued exploration into retroviruses' role in schizophrenia could illuminate the disorder's pathogenic mechanisms. In our research, clinical data found that GPX4 and SLC3A2, potential serum-based biomarkers, were inversely correlated with ERVW-1. Our in-depth study suggested that ERVW-1 can promote ferroptosis by downregulating the expression of GPX4 and SLC3A2, which may indicate a novel mechanism by which ERVW-1 affects neural cell death in schizophrenia.

The course and pathophysiology of schizophrenia are complex, diverse, and affected by many environmental and epigenetic factors (Hung et al., 2021). However, its gene therapy approach is challenging and limited, and accurate diagnosis and treatment are problematic (Marder et al., 2019). Therefore, it is essential to investigate the specific mechanisms and biomarkers of schizophrenia. In the era of big data, GEO databases have become a crucial tool for studying disease mechanisms. In this study, we screened the schizophrenia-related dataset GSE53987 in the GEO database and performed bioinformatics analysis and enrichment analysis. Our analysis of the transcriptional profile of GSE53987 revealed widespread inflammation in schizophrenia (Lanz et al., 2019). In addition, our KEGG analysis of GSE53987 revealed that DEGs were related to the ferroptosis pathway. Other enriched pathways, such as glutamatergic synapses, the p53 signaling pathway, and fatty acid metabolism, were also associated with ferroptosis. The enrichment analysis results of GO biological processes comprised lipid metabolic processes, metal ion homeostasis, mitochondrial transport, and cellular response to oxygen levels, which overlapped with ferroptosis. These results suggested that ferroptosis-related genes might influence the progression of schizophrenia via the aforementioned processes, suggesting ferroptosis's potential link to the pathophysiology of schizophrenia.

Our bioinformatics analysis and clinical results suggested that the GPX4 gene was lowly expressed in schizophrenia and negatively correlated with ERVW-1. GPX4 plays an essential role in a variety of neurological diseases (Cardoso et al., 2017), including the survival of interneurons and the prevention of seizures, and it prevents neurodegeneration by inhibiting ferroptosis (Reichert et al., 2020). Additionally, GPX4 is associated with the occurrence and development of various diseases. Research shows that GPX4 has low activity in tissue samples of patients with Krohn's disease (Mayr et al., 2020). Its expression level significantly increases in tumor tissues, including lung adenocarcinoma, prostate cancer, rectal cancer adenocarcinoma, thyroid cancer, and endometrial cancer (Zhang et al., 2020). Furthermore, the synthesis of GSH through cystine/glutamic transport system Xc-is the limiting step of GPX4 detoxification lipid peroxide function (Reichert et al., 2020). Our clinical data indicated that SLC3A2 was significantly downregulated and negatively correlated with ERVW-1 in schizophrenia patients. Previous studies show that SLC3A2 mRNA expression in peripheral leukocytes is lower in patients with schizophrenia than in healthy individuals (Lin et al., 2016). This aligns with our findings from clinical samples and supports the hypothesis of impaired aminergic neurotransmission underlying pathophysiology of schizophrenia.

Ferroptosis is a unique form of cell death caused by lipid peroxide produced and the oxidation of active substances produced by free iron. Previous studies have shown that ferroptosis is closely related to various neuropsychiatric diseases, including Alzheimer's disease (Bao et al., 2021), Parkinson's disease (Wang et al., 2022), and Huntington's disease (Weiland et al., 2019). Additionally, viral infections can induce ferroptosis. For example, herpes simplex virus type 1 (HSV-1) induces ferroptosis in viral encephalitis (Xu et al., 2023). However, there is no research on the relationship between ferroptosis and schizophrenia. The mechanisms of ferroptosis in various neurological diseases are mainly due to intracellular iron accumulation, depletion of glutathione (GSH),

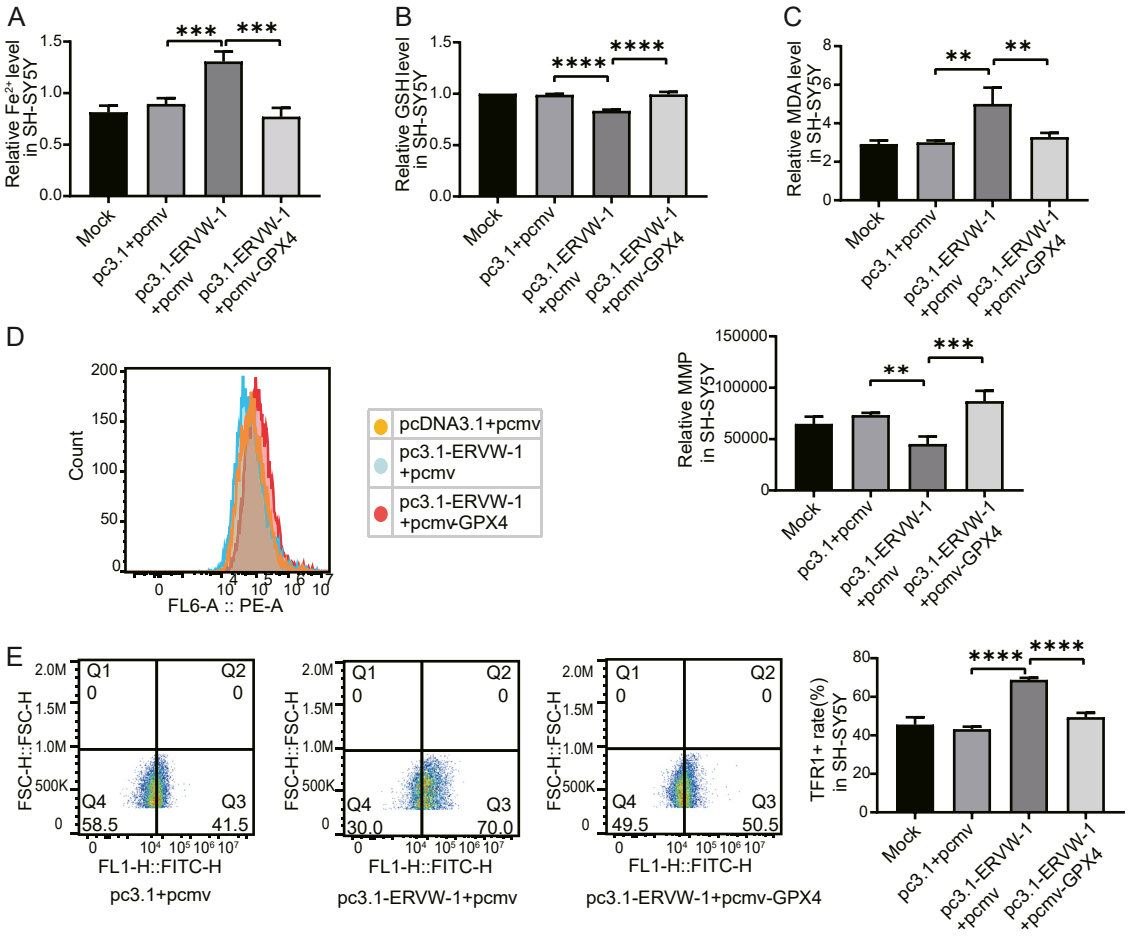

Fig. 5. ERVW-1 induced ferroptosis through GPX4. The Fe^{2+} (**A**), GSH (**B**), MDA (**C**), mitochondrial membrane potential (**D**), and TFR1 (**E**) levels in SH-SY5Y cells after co-transfection with ERVW-1 and GPX4. Data shown are mean ± SD. $^{**}P < 0.01$, $^{***}P < 0.001$, $^{****}P < 0.0001$; one-way ANOVA.

blockade of the system Xc-, inhibition of GPX4, or lipid peroxidation (Weiland et al., 2019). As our clinical results showed that ERVW-1 had a high correlation with ferroptosis-related genes GPX4 and SLC3A2 in schizophrenia, we investigated the effect of ERVW-1 on ferroptosis in cytological experiments. The detection of markers of ferroptosis has been a critical advance in the study of ferroptosis. There are four leading points of ferroptosis: lipid peroxidation, mitochondria damage, specific gene expression changes, and upregulation of TFR1 (Stockwell, 2022). Our results suggested that ERVW-1 induced ferroptosis and promoted lipid peroxidation. A few studies report that ferroptosis and lipid peroxidation may lead to inflammation and DNA changes, and trigger premature aging, functional degradation, and death of neurons (Mao et al., 2020; Reichert et al., 2020). The oxidative stress and antioxidant imbalance inflicting neuronal damage may be pivotal to schizophrenia's etiology (Bryll et al., 2020). Our findings offer insights into a potential mechanism through which ERVW-1 modulates neuronal cell death in schizophrenia.

Cells have evolved various defense mechanisms to detoxify toxic lipid peroxides, the most prominent of which is GPX4. GPX4 is a selenoprotein in mammals that repairs oxidative lipid damage in cells by directly reducing toxic lipid peroxides (PL-OOH) to non-toxic lipid alcohols (PL-OH) using reduced glutathione (GSH) as a substrate (Ursini et al., 2020). Furthermore, since intracellular oxidative stress and excitotoxicity are vital factors associated with the neurodegenerative processes, the system Xc-regulating glutathione and glutamate is thought to be essential in the pathogenesis of many central nervous system diseases (Sheldon et al., 2007). The protein subunit system Xc-, related to glutamate, is composed of heavy chain subunit 4F2hc, solute carrier (SLC) family 3 member 2 (SLC3A2), light chain subunit xCT and SLC family 7 member 11 (SLC7A11) (Zhang et al., 2022). It is primarily responsible for the cellular uptake of cystine in exchange for intracellular glutamate, a process that ultimately leads to cysteine production within system Xc-. Cysteine is the rate-limiting substrate for the biosynthesis of the antioxidant glutathione (GSH), one of the significant antioxidants for the brain (Koppula et al., 2021). The effect of system Xc-on the intracellular concentration of human brain cells is crucial in regulating many neurotransmitter pathways. Inhibition of system Xc-causes a rapid decrease of intracellular glutathione levels and cell death caused by the accumulation of lipogenic ROS. Our results showed that ERVW-1 could reduce the expression of GPX4 and SLC3A2. In addition, ERVW-1 may affect the promoter activity of some genes (Xia et al., 2021; Yao et al., 2023). We predicted the active sites of GPX4 and SLC3A2 promoters by Promoter 2.0 Prediction, TSSG, and TSSW, and the results showed that the potential active site of the GPX4 promoter could be located within the region of −200 to −50 and the active site of the SLC3A2 promoter might be between −190 and −40 region. We then designed four truncated promoters and ligated them with the promoter-reporter vector pGL3-basic for luciferase experiments. Luciferase assay showed that the GPX4 promoter activity from the −300 to +100 region surpassed that of the −100 to +100 region. Moreover, the influence of ERVW-1 on the GPX4 promoter from the −100 to +100

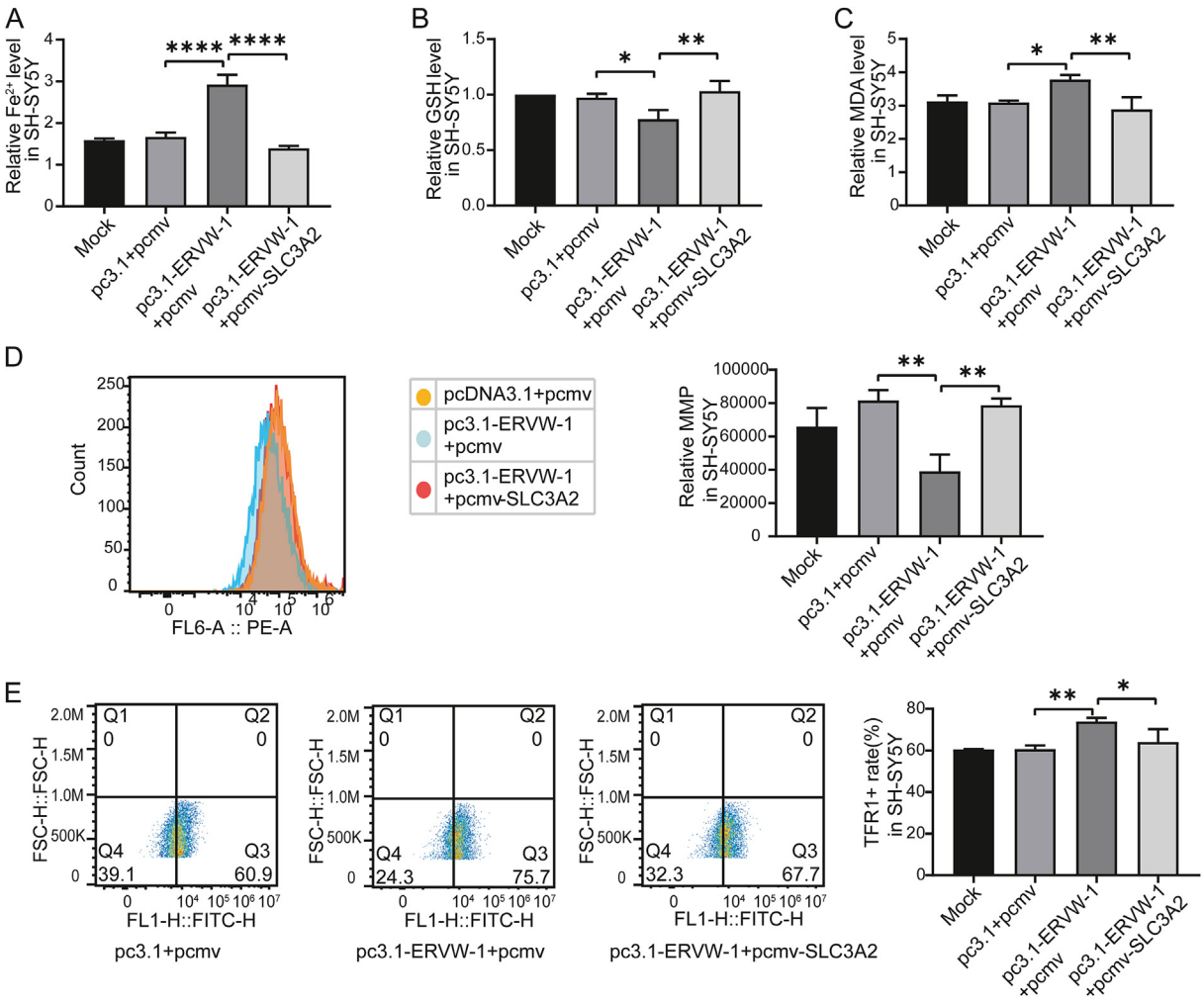

Fig. 6. ERVW-1 induced ferroptosis through SLC3A2. The Fe^{2+} (**A**), GSH (**B**), MDA (**C**), mitochondrial membrane potential (**D**), and TFR1 (**E**) levels in SH-SY5Y cells after co-transfection with ERVW-1 and SLC3A2. Data shown are mean ± SD. $^{*}P < 0.05$, $^{**}P < 0.01$, $^{***}P < 0.001$; one-way ANOVA.

region was not significantly different from the control group. Thus, the region, from −300 to −100 is essential for ERVW-1-suppressed GPX4 expression. Similarly, the −188 to +12 region is critical for ERVW-1-mediated suppression of SLC3A2 expression. Besides, our results demonstrated that SLC3A2 could reverse the inhibitory effect of ERVW-1 on GPX4 transcription. Previous studies have indicated that the depletion of GSH can hinder the activation of signal transducer and activator of transcription 3 (STAT3) in cells (Liang et al., 2018), which in turn regulates the activation of GPX4 (Zhang et al., 2022). SLC3A2 mediates GSH synthesis, potentially facilitating the activation of STAT3 and consequently promoting the transcription of GPX4. However, the precise mechanism behind this phenomenon necessitates further elucidation through experimental investigations.

The System Xc-/GSH/GPX4 pathway is the primary cellular antioxidant against ferroptosis (Liu et al., 2022). System Xc-inhibition downregulates intracellular GSH, resulting in an inhibitory effect on GPX4 (Ursini et al., 2020). Viral infection inhibits the GPX4-dependent pathway to regulate ferroptosis, promoting its replication, spread, and pathogenesis. Severe acute respiratory syndrome coronavirus 2 (SARS-CoV-2) induces ferroptosis to replicate or spread by inhibiting the expression of GSH or GPX4 (Han et al., 2022). Epstein-Barr virus (EBV) can inhibit ferroptosis by promoting the transcription factor nuclear factor erythroid 2-related factor 2 (NRF2) upstream of GPX4 and promote the occurrence of EBV-related tumors (Yuan et al., 2022). Hepatitis B virus protein X (HBx) downregulates SLC7A11 to promote ferroptosis of hepatocytes, leading to acute liver injury (Liu et al., 2021). Our results showed that GPX4 and SLC3A2 reversed the promotion of ferroptosis induced by ERVW-1. Therefore, we proposed that ERVW-1 contributed to ferroptosis by downregulating the expression of GPX4 and SLC3A2.

Fer-1 is a synthetic compound identified as a ferroptosis inhibitor isolated through high-throughput screening of small molecular libraries (Dixon et al., 2012). Studies have shown that the anti-ferroptosis activity of fer-1 is actually due to the scavenging of initiating alkoxyl radicals produced, together with other rearrangement products, by ferrous iron from lipid hydroperoxides (Miotto et al., 2020). Besides, studies have shown that Coxsackievirus A6 (CV-A6) infection-induced ferroptosis via ACSL4 leads to excessive lipid ROS. At the same time, Fer-1 can suspend the formation of viral replication organelles and lipid ROS levels, thereby inhibiting the replication of CV-A6 (Kung et al., 2022). We detected the ferroptosis indexes after adding Fer-1. Moreover, we found that Fer-1 could significantly reverse the impact of ERVW-1 on ferroptosis-related markers. The above results indicated that Fer-1 could inhibit ferroptosis indexes induced by ERVW-1, solidifying the notion that ERVW-1 induced ferroptosis.

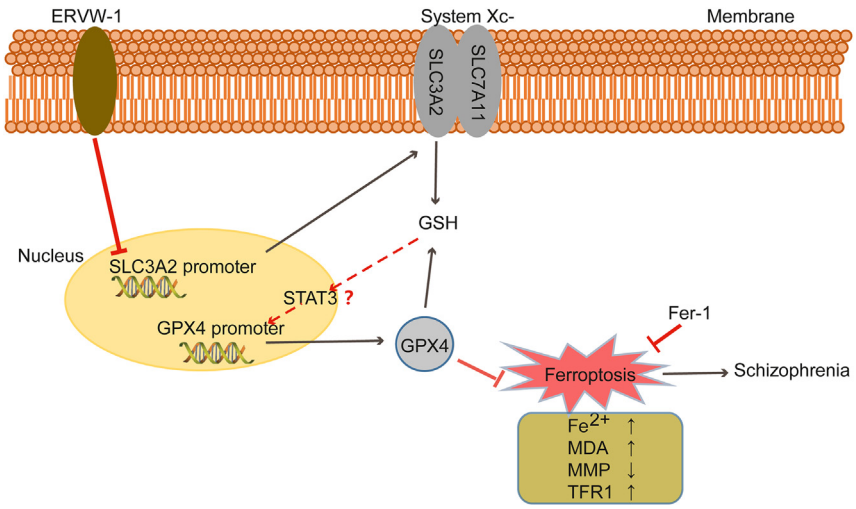

Fig. 7. ERVW-1 promoted ferroptosis by downregulating the expression of GPX4 and SLC3A2. ERVW-1 decreased the GSH level and mitochondrial membrane potential, and increased the level of Fe^{2+}, MDA, and TFR1, which are indicators of ferroptosis. Ferrostatin-1 (Fer-1) could inhibit the effect induced by ERVW-1. ERVW-1 promoted ferroptosis by downregulating the expression of GPX4 and SLC3A2, which might indicate a new mechanism of ERVW-1 on neuronal damage in schizophrenia.

5. Conclusions

Our clinical observations showed that serum GPX4 and SLC3A2 levels were diminished in patients with schizophrenia than in healthy controls and inversely correlated with ERVW-1. *In vitro* experiments have shown that ERVW-1 can inhibit promoter activity of GPX4 and SLC3A2, thereby reducing GPX4 and SLC3A2 expression. In addition, ERVW-1 induced visible changes in the levels of Fe^{2+}, the expression of GSH, MDA, and TFR1, as well as alterations in mitochondrial membrane potential hallmarks of ferroptosis. Subsequent investigations confirmed that these pivotal ferroptosis markers significantly improved in the presence of Fer-1. In conclusion, ERVW-1 fostered ferroptosis by attenuating the expression of GPX4 and SLC3A2 in neurons. This revelation potentially uncovered a novel ERVW-1-driven mechanism underlying neuronal damage and offered a fresh perspective for understanding the etiology of schizophrenia (Fig. 7).

Data availability

All data generated or analyzed during this study are included in this published article.

Ethics statement

The study was approved by the Ethics Committee of the School of Medicine of Wuhan University (grant #06R-1366). The collection of blood samples in this study followed the principles of the Helsinki Declaration, and obtained informed written consent from all subjects.

Author contributions

Dongyan Zhang: investigation, data curation, methodology, and writing-original draft. Xiulin Wu: data curation and validation. Xing Xue: software. Wenshi Li: formal analysis. Ping Zhou: formal analysis and supervision. Zhao Lv: methodology. Kexin Zhao: formal analysis. Fan Zhu: conceptualization, project administration, and writing (review and editing).

Conflict of interest

All authors declare that they have no competing interests.

Acknowledgements

This work was supported by the National Natural Science Foundation of China (Nos. 82272321 and 81971943), Fundamental Research Funds for the Central Universities (2042023kf0230), and the Stanley Foundation from the Stanley Medical Research Institute (SMRI), United States (No.06R-1366). We acknowledge the Medicine Research Center for Structural Biology of Wuhan University for providing the flow cytometer (Beckman Coulter, Miami, FL, USA). We thank the contributor for providing the data set of human schizophrenia, whose registration number is GSE53987 (http://www.ncbi.nlm.nih.gov/geo). We thank the Renmin Hospital, Wuhan University for providing blood samples from schizophrenics and healthy people.

Appendix A. Supplementary data

Supplementary data to this article can be found online at https://doi.org/10.1016/j.virs.2023.09.001.

References

American Psychiatric Association, 2013. Diagnostic and statistical manual of mental disorders. 5th ed. American Psychiatric Publishing, Inc.
Bao, W.D., Pang, P., Zhou, X.T., Hu, F., Xiong, W., Chen, K., Wang, J., Wang, F., Xie, D., Hu, Y.Z., et al., 2021. Loss of ferroportin induces memory impairment by promoting ferroptosis in Alzheimer's disease. Cell Death Differ. 28, 1548–1562.
Bridges, R.J., Natale, N.R., Patel, S.A., 2012. System xc(-) cystine/glutamate antiporter: an update on molecular pharmacology and roles within the CNS. Br. J. Pharmacol. 165, 20–34.
Bryll, A., Skrzypek, J., Krzysciak, W., Szelagowska, M., Smierciak, N., Kozicz, T., Popiela, T., 2020. Oxidative-antioxidant imbalance and impaired glucose metabolism in schizophrenia. Biomolecules 10, 384.
Canadas, I., Thummalapalli, R., Kim, J.W., Kitajima, S., Jenkins, R.W., Christensen, C.L., Campisi, M., Kuang, Y., Zhang, Y., Gjini, E., et al., 2018. Tumor innate immunity primed by specific interferon-stimulated endogenous retroviruses. Nat. Med. 24, 1143–1150.
Cardoso, B.R., Hare, D.J., Bush, A.I., Roberts, B.R., 2017. Glutathione peroxidase 4: a new player in neurodegeneration? Mol. Psychiatr. 22, 328–335.
Chen, Y., Yan, Q., Zhou, P., Li, S., Zhu, F., 2019. HERV-W env regulates calcium influx via activating TRPC3 channel together with depressing DISC1 in human neuroblastoma cells. J. Neurovirol. 25, 101–113.
Danino, Y.M., Even, D., Ideses, D., Juven-Gershon, T., 2015. The core promoter: at the heart of gene expression. Biochim. Biophys. Acta 1849, 1116–1131.
Dixon, S.J., Lemberg, K.M., Lamprecht, M.R., Skouta, R., Zaitsev, E.M., Gleason, C.E., Patel, D.N., Bauer, A.J., Cantley, A.M., Yang, W.S., et al., 2012. Ferroptosis: an iron-dependent form of nonapoptotic cell death. Cell 149, 1060–1072.

Garcia-Montojo, M., Doucet-O'Hare, T., Henderson, L., Nath, A., 2018. Human endogenous retrovirus-K (HML-2): a comprehensive review. Crit. Rev. Microbiol. 44, 715–738.
Garcia-Montojo, M., Rodriguez-Martin, E., Ramos-Mozo, P., Ortega-Madueno, I., Dominguez-Mozo, M.I., Arias-Leal, A., Garcia-Martinez, M.A., Casanova, I., Galan, V., Arroyo, R., et al., 2020. Syncytin-1/HERV-W envelope is an early activation marker of leukocytes and is upregulated in multiple sclerosis patients. Eur. J. Immunol. 50, 685–694.
Geis, F.K., Goff, S.P., 2020. Silencing and transcriptional regulation of endogenous retroviruses: an overview. Viruses-Basel 12, 884.
Gifford, R.J., Blomberg, J., Coffin, J.M., Fan, H., Heidmann, T., Mayer, J., Stoye, J., Tristem, M., Johnson, W.E., 2018. Nomenclature for endogenous retrovirus (ERV) loci. Retrovirology 15, 59.
Grandi, N., Tramontano, E., 2018a. Human endogenous retroviruses are ancient acquired elements still shaping innate immune responses. Front. Immunol. 9, 2039.
Grandi, N., Tramontano, E., 2018b. HERV envelope proteins: physiological role and pathogenic potential in cancer and autoimmunity. Front. Microbiol. 9, 462.
Han, Y., Zhu, J., Yang, L., Nilsson-Payant, B.E., Hurtado, R., Lacko, L.A., Sun, X., Gade, A.R., Higgins, C.A., Sisso, W.J., et al., 2022. SARS-CoV-2 infection induces ferroptosis of sinoatrial node pacemaker cells. Circ. Res. 130, 963–977.
Huang, W., Li, S., Hu, Y., Yu, H., Luo, F., Zhang, Q., Zhu, F., 2011. Implication of the env gene of the human endogenous retrovirus W family in the expression of BDNF and DRD3 and development of recent-onset schizophrenia. Schizophr. Bull. 37, 988–1000.
Hung, C.C., Lin, C.H., Lane, H.Y., 2021. Cystine/glutamate antiporter in schizophrenia: from molecular mechanism to novel biomarker and treatment. Int. J. Mol. Sci. 22, 9718.
Illescas-Montes, R., Corona-Castro, C.C., Melguizo-Rodriguez, L., Ruiz, C., Costela-Ruiz, V.J., 2019. Infectious processes and systemic lupus erythematosus. Immunology 158, 153–160.
Jansz, N., Faulkner, G.J., 2021. Endogenous retroviruses in the origins and treatment of cancer. Genome Biol. 22, 147.
Jiang, X., Stockwell, B.R., Conrad, M., 2021. Ferroptosis: mechanisms, biology and role in disease. Nat. Rev. Mol. Cell Biol. 22, 266–282.
Koppula, P., Zhuang, L., Gan, B., 2021. Cystine transporter SLC7A11/xCT in cancer: ferroptosis, nutrient dependency, and cancer therapy. Protein Cell 12, 599–620.
Kourou, K., Exarchos, T.P., Exarchos, K.P., Karamouzis, M.V., Fotiadis, D.I., 2015. Machine learning applications in cancer prognosis and prediction. Comput Struct Biotec 13, 8–17.
Kung, Y.A., Chiang, H.J., Li, M.L., Gong, Y.N., Chiu, H.P., Hung, C.T., Huang, P.N., Huang, S.Y., Wang, P.Y., Hsu, T.A., et al., 2022. Acyl-coenzyme A synthetase long-chain family member 4 is involved in viral replication organelle formation and facilitates virus replication via ferroptosis. mBio 13, e271721.
Kury, P., Nath, A., Creange, A., Dolei, A., Marche, P., Gold, J., Giovannoni, G., Hartung, H.P., Perron, H., 2018. Human endogenous retroviruses in neurological diseases. Trends Mol. Med. 24, 379–394.
Lanz, T.A., Reinhart, V., Sheehan, M.J., Rizzo, S., Bove, S.E., James, L.C., Volfson, D., Lewis, D.A., Kleiman, R.J., 2019. Postmortem transcriptional profiling reveals widespread increase in inflammation in schizophrenia: a comparison of prefrontal cortex, striatum, and hippocampus among matched tetrads of controls with subjects diagnosed with schizophrenia, bipolar or major depressive disorder. Transl. Psychiatry 9, 151.
Lee, J.R., Ahn, K., Kim, Y.J., Jung, Y.D., Kim, H.S., 2012. Radiation-induced human endogenous retrovirus (HERV)-R env gene expression by epigenetic control. Radiat. Res. 178, 379–384.
Li, S., Liu, Z.C., Yin, S.J., Chen, Y.T., Yu, H.L., Zeng, J., Zhang, Q., Zhu, F., 2013. Human endogenous retrovirus W family envelope gene activates the small conductance Ca^{2+}-activated K^{+} channel in human neuroblastoma cells through CREB. Neuroscience 247, 164–174.
Li, X., Wu, X., Li, W., Yan, Q., Zhou, P., Xia, Y., Yao, W., Zhu, F., 2023. HERV-W ENV induces innate immune activation and neuronal apoptosis via linc01930/cGAS Axis in recent-onset schizophrenia. Int. J. Mol. Sci. 24, 3000.
Li, Y., Zhang, G., Cui, J., 2022. Origin and deep evolution of human endogenous retroviruses in pan-primates. Viruses-Basel 14, 1370.
Liang, J., Jahraus, B., Balta, E., Ziegler, J.D., Hubner, K., Blank, N., Niesler, B., Wabnitz, G.H., Samstag, Y., 2018. Sulforaphane inhibits inflammatory responses of primary human T-cells by increasing ROS and depleting glutathione. Front. Immunol. 9, 2584.
Lin, C.H., Lin, P.P., Lin, C.Y., Lin, C.H., Huang, C.H., Huang, Y.J., Lane, H.Y., 2016. Decreased mRNA expression for the two subunits of system xc(-), SLC3A2 and SLC7A11, in WBC in patients with schizophrenia: evidence in support of the hypo-glutamatergic hypothesis of schizophrenia. J. Psychiatr. Res. 72, 58–63.
Liu, C., Chen, Y., Li, S., Yu, H., Zeng, J., Wang, X., Zhu, F., 2013. Activation of elements in HERV-W family by caffeine and aspirin. Virus Gene. 47, 219–227.
Liu, C., Liu, L., Wang, X., Liu, Y., Wang, M., Zhu, F., 2017. HBV X Protein induces overexpression of HERV-W env through NF-kappaB in HepG2 cells. Virus Gene. 53, 797–806.
Liu, G.Z., Xu, X.W., Tao, S.H., Gao, M.J., Hou, Z.H., 2021. HBx facilitates ferroptosis in acute liver failure via EZH2 mediated SLC7A11 suppression. J. Biomed. Sci. 28, 67.
Liu, J., Kang, R., Tang, D., 2022. Signaling pathways and defense mechanisms of ferroptosis. FEBS J. 289, 7038–7050.
Mameli, G., Astone, V., Arru, G., Marconi, S., Lovato, L., Serra, C., Sotgiu, S., Bonetti, B., Dolei, A., 2007. Brains and peripheral blood mononuclear cells of multiple sclerosis (MS) patients hyperexpress MS-associated retrovirus/HERV-W endogenous retrovirus, but not Human herpesvirus 6. J. Gen. Virol. 88, 264–274.
Mao, H., Zhao, Y., Li, H., Lei, L., 2020. Ferroptosis as an emerging target in inflammatory diseases. Prog. Biophys. Mol. Biol. 155, 20–28.
Mao, J., Zhang, Q., Cong, Y.S., 2021. Human endogenous retroviruses in development and disease. Comput Struct Biotec 19, 5978–5986.
Marder, S.R., Cannon, T.D., 2019. Schizophrenia. N. Engl. J. Med. 381, 1753–1761.
Markovitz, D.M., 2014. "Reverse genomics" and human endogenous retroviruses. Trans. Am. Clin. Climatol. Assoc. 125, 57–62.
Mayr, L., Grabherr, F., Schwarzler, J., Reitmeier, I., Sommer, F., Gehmacher, T., Niederreiter, L., He, G.W., Ruder, B., Kunz, K., et al., 2020. Dietary lipids fuel GPX4-restricted enteritis resembling Crohn's disease. Nat. Commun. 11, 1775.
Miotto, G., Rossetto, M., Di Paolo, M.L., Orian, L., Venerando, R., Roveri, A., Vuckovic, A.M., Bosello, T.V., Zaccarin, M., Zennaro, L., et al., 2020. Insight into the mechanism of ferroptosis inhibition by ferrostatin-1. Redox Biol. 28, 101328.
Mohammadi, A., Rashidi, E., Amooeian, V.G., 2018. Brain, blood, cerebrospinal fluid, and serum biomarkers in schizophrenia. Psychiatr. Res. 265, 25–38.
Nevalainen, T., Autio, A., Mishra, B.H., Marttila, S., Jylha, M., Hurme, M., 2018. Aging-associated patterns in the expression of human endogenous retroviruses. PLoS One 13, e207407.
Posso-Osorio, I., Tobon, G.J., Canas, C.A., 2021. Human endogenous retroviruses (HERV) and non-HERV viruses incorporated into the human genome and their role in the development of autoimmune diseases. J Transl Autoimmun 4, 100137.
Reichert, C.O., de Freitas, F.A., Sampaio-Silva, J., Rokita-Rosa, L., Barros, P.D.L., Levy, D., Bydlowski, S.P., 2020a. Ferroptosis mechanisms involved in neurodegenerative diseases. Int. J. Mol. Sci. 21, 8765.
Reichert, C.O., de Freitas, F.A., Sampaio-Silva, J., Rokita-Rosa, L., Barros, P.L., Levy, D., Bydlowski, S.P., 2020b. Ferroptosis mechanisms involved in neurodegenerative diseases. Int. J. Mol. Sci. 21, 8765.
Sheldon, A.L., Robinson, M.B., 2007. The role of glutamate transporters in neurodegenerative diseases and potential opportunities for intervention. Neurochem. Int. 51, 333–355.
Shen, W., Song, Z., Zhong, X., Huang, M., Shen, D., Gao, P., Qian, X., Wang, M., He, X., Wang, T., et al., 2022. Sangerbox: a comprehensive, interaction-friendly clinical bioinformatics analysis platform. iMeta 1, e36.
Song, Y., Li, X., Wei, X., Cui, J., 2021. Human endogenous retroviruses as biomedicine markers. Virol. Sin. 36, 852–858.
Stepnicki, P., Kondej, M., Kaczor, A.A., 2018. Current concepts and treatments of schizophrenia. Molecules 23, 2087.
Stockwell, B.R., 2022. Ferroptosis turns 10: emerging mechanisms, physiological functions, and therapeutic applications. Cell 185, 2401–2421.
Tandon, R., Gaebel, W., Barch, D.M., Bustillo, J., Gur, R.E., Heckers, S., Malaspina, D., Owen, M.J., Schultz, S., Tsuang, M., et al., 2013. Definition and description of schizophrenia in the DSM-5. Schizophr. Res. 150, 3–10.
Tang, W., Guo, J., Liu, W., Ma, J., Xu, G., 2021. Ferrostatin-1 attenuates ferroptosis and protects the retina against light-induced retinal degeneration. Biochem Bioph Res Co 548, 27–34.
Tu, X., Li, S., Zhao, L., Xiao, R., Wang, X., Zhu, F., 2017. Human leukemia antigen-A*0201-restricted epitopes of human endogenous retrovirus W family envelope (HERV-W env) induce strong cytotoxic T lymphocyte responses. Virol. Sin. 32, 280–289.
Ursini, F., Maiorino, M., 2020. Lipid peroxidation and ferroptosis: the role of GSH and GPx4. Free Radic. Biol. Med. 152, 175–185.
Vargiu, L., Rodriguez-Tome, P., Sperber, G.O., Cadeddu, M., Grandi, N., Blikstad, V., Tramontano, E., Blomberg, J., 2016. Classification and characterization of human endogenous retroviruses; mosaic forms are common. Retrovirology 13, 7.
Vection, S., O'Callaghan, D., Keriel, A., 2022. CD98hc in host-pathogen interactions: roles of the multifunctional host protein during infections. FEMS Microbiol. Rev. 46, fuac023.
Wang, X., Huang, J., Zhu, F., 2018a. Human endogenous retroviral envelope protein syncytin-1 and inflammatory abnormalities in neuropsychological diseases. Front. Psychiatr. 9, 422.
Wang, X., Liu, Z., Wang, P., Li, S., Zeng, J., Tu, X., Yan, Q., Xiao, Z., Pan, M., Zhu, F., 2018b. Syncytin-1, an endogenous retroviral protein, triggers the activation of CRP via TLR3 signal cascade in glial cells. Brain Behav. Immun. 67, 324–334.
Wang, X., Wu, X., Huang, J., Li, H., Yan, Q., Zhu, F., 2021. Human endogenous retrovirus W family envelope protein (HERV-W env) facilitates the production of TNF-alpha and IL-10 by inhibiting MyD88s in glial cells. Arch. Virol. 166, 1035–1045.
Wang, Y., Chen, G., Shao, W., 2022a. Identification of ferroptosis-related genes in Alzheimer's disease based on bioinformatic analysis. Front Neurosci-Switz 16, 823741.
Wang, Z.L., Yuan, L., Li, W., Li, J.Y., 2022b. Ferroptosis in Parkinson's disease: glia-neuron crosstalk. Trends Mol. Med. 28, 258–269.
Weiland, A., Wang, Y., Wu, W., Lan, X., Han, X., Li, Q., Wang, J., 2019. Ferroptosis and its role in diverse brain diseases. Mol. Neurobiol. 56, 4880–4893.
Wu, X., Yan, Q., Liu, L., Xue, X., Yao, W., Li, X., Li, W., Ding, S., Xia, Y., Zhang, D., Zhu, F., 2023. Domesticated HERV-W env contributes to the activation of the small conductance Ca^{2+}-activated K^{+} type 2 channels via decreased 5-HT4 receptor in recent-onset schizophrenia. Virol. Sin. 38, 9–22.
Xia, Y.R., Wei, X.C., Li, W.S., Yan, Q.J., Wu, X.L., Yao, W., Li, X.H., Zhu, F., 2021. CPEB1, a novel risk gene in recent-onset schizophrenia, contributes to

mitochondrial complex I defect caused by a defective provirus ERVWE1. World J. Psychiatr. 11, 1075–1094.
Xiao, R., Li, S., Cao, Q., Wang, X., Yan, Q., Tu, X., Zhu, Y., Zhu, F., 2017. Human endogenous retrovirus W env increases nitric oxide production and enhances the migration ability of microglia by regulating the expression of inducible nitric oxide synthase. Virol. Sin. 32, 216–225.
Xu, X.Q., Xu, T., Ji, W., Wang, C., Ren, Y., Xiong, X., Zhou, X., Lin, S.H., Xu, Y., Qiu, Y., 2023. Herpes simplex virus 1-induced ferroptosis contributes to viral encephalitis. mBio 14, e237022.
Xue, X., Wu, X., Liu, L., Liu, L., Zhu, F., 2023. ERVW-1 activates ATF6-mediated unfolded protein response by decreasing GANAB in recent-onset schizophrenia. Viruses-Basel 15, 1298.
Yan, H.F., Zou, T., Tuo, Q.Z., Xu, S., Li, H., Belaidi, A.A., Lei, P., 2021. Ferroptosis: mechanisms and links with diseases. Signal Transduct Tar 6, 49.
Yan, Q., Wu, X., Zhou, P., Zhou, Y., Li, X., Liu, Z., Tan, H., Yao, W., Xia, Y., Zhu, F., 2022. HERV-W envelope triggers abnormal dopaminergic neuron process through DRD2/PP2A/AKT1/GSK3 for schizophrenia risk. Viruses-Basel 14, 145.
Yao, W., Zhou, P., Yan, Q., Wu, X., Xia, Y., Li, W., Li, X., Zhu, F., 2023. ERVWE1 reduces hippocampal neuron density and impairs dendritic spine morphology through inhibiting Wnt/JNK non-canonical pathway via miR-141-3p in schizophrenia. Viruses-Basel 15, 168.
Yu, H.L., Zhao, Z.K., Zhu, F., 2013. The role of human endogenous retroviral long terminal repeat sequences in human cancer. Int. J. Mol. Med. 32, 755–762.
Yu, H., Liu, T., Zhao, Z., Chen, Y., Zeng, J., Liu, S., Zhu, F., 2014. Mutations in 3'-long terminal repeat of HERV-W family in chromosome 7 upregulate syncytin-1 expression in urothelial cell carcinoma of the bladder through interacting with c-Myb. Oncogene 33, 3947–3958.
Yuan, L., Li, S., Chen, Q., Xia, T., Luo, D., Li, L., Liu, S., Guo, S., Liu, L., Du, C., et al., 2022. EBV infection-induced GPX4 promotes chemoresistance and tumor progression in nasopharyngeal carcinoma. Cell Death Differ. 29, 1513–1527.
Zhang, Q., Pan, J., Cong, Y., Mao, J., 2022a. Transcriptional regulation of endogenous retroviruses and their misregulation in human diseases. Int. J. Mol. Sci. 23, 10112.
Zhang, W., Gong, M., Zhang, W., Mo, J., Zhang, S., Zhu, Z., Wang, X., Zhang, B., Qian, W., Wu, Z., et al., 2022b. Thiostrepton induces ferroptosis in pancreatic cancer cells through STAT3/GPX4 signalling. Cell Death Dis. 13, 630.
Zhang, X., Sui, S., Wang, L., Li, H., Zhang, L., Xu, S., Zheng, X., 2020. Inhibition of tumor propellant glutathione peroxidase 4 induces ferroptosis in cancer cells and enhances anticancer effect of cisplatin. J. Cell. Physiol. 235, 3425–3437.
Zhang, X., Zheng, C., Gao, Z., Chen, H., Li, K., Wang, L., Zheng, Y., Li, C., Zhang, H., Gong, M., et al., 2022c. SLC7A11/xCT prevents cardiac hypertrophy by inhibiting ferroptosis. Cardiovasc. Drugs Ther. 36, 437–447.
Zhang, Y., Lu, Y., Jin, L., 2022d. Iron metabolism and ferroptosis in physiological and pathological pregnancy. Int. J. Mol. Sci. 23, 9395.
Zhang, Y., Xin, L., Xiang, M., Shang, C., Wang, Y., Wang, Y., Cui, X., Lu, Y., 2022e. The molecular mechanisms of ferroptosis and its role in cardiovascular disease. Biomed. Pharmacother. 145, 112423.
Zhou, B., Qi, F., Wu, F., Nie, H., Song, Y., Shao, L., Han, J., Wu, Z., Saiyin, H., Wei, G., et al., 2019. Endogenous retrovirus-derived long noncoding RNA enhances innate immune responses via derepressing RELA expression. mBio 10, e00937, 19.
Zhou, Y., Liu, L., Liu, Y., Zhou, P., Yan, Q., Yu, H., Chen, X., Zhu, F., 2021. Implication of human endogenous retrovirus W family envelope in hepatocellular carcinoma promotes MEK/ERK-mediated metastatic invasiveness and doxorubicin resistance. Cell Death Dis. 7, 177.